Simulation and Analysis for a Model of Excitation/Deexcitation and Ionization/Recombination in a Plasma *

Farzin Barekat† and Russel Caflisch† and Jean-Luc Cambier‡ and Bokai Yan†

January 21, 2014

Abstract

This paper describes a Monte Carlo simulation method for excitation/deexcitation and ionization/recombination in a plasma. The atoms and ions in the plasma are represented by continuum densities and the electrons by a particle distribution. The wide range of kinetic rates for these processes leads to computational bottlenecks that are overcome by development of acceleration techniques. The simulation method is developed for an idealized analytic model of the excitation and ionization energetic cross sections. Numerical results are presented to demonstrate the efficiency of the method on spatially homogeneous problems. The results are compared to the semi-analytic results from a rate equation approach.

1 Introduction

Simulation of plasma dynamics can be computationally challenging due to the large number of physical processes and the wide range of space/time scales over which they operate. This is particularly true of kinetic processes such as excitation (and deexcitation) and ionization (and recombination). The relative significance of these particle interactions is measured by the Knudsen number $Kn = L_c/L_0$, in which L_c is the mean free path between collisions and L_0 is a characteristic length scale. In the limit of small Knudsen number, the velocity (or energy) distribution function f for each of the particle species goes to a Maxwellian equilibrium, and the evolution of f can be described by fluid-like equations, in which individual particle interactions do not need to be resolved. On the other hand, individual interactions are significant for finite Knudsen number, so that a particle representation and a Monte Carlo simulation procedure are appropriate.

This paper describes the development of a particle simulation method for plasma kinetics, including excitation and ionization, and investigation of acceleration strategies for this simulation method. We first review the mathematical description of excitation/deexcitation and ionization/recombination, in terms of the differential cross sections for each process. In particular, the principle of detailed balance is used to derive the deexcitation cross section from the excitation cross section and the recombination cross section from the ionization cross section. We also formulate a Boltzmann equation for the evolution of the electron distribution and the atom and ion densities. Using the Boltzmann equation, we formulate and derive a version of Boltzmann's H-Theorem for excitation/deexcitation and ionization/recombination. Although not unexpected, the H function is new in this context to the best of our knowledge.

As a scientific platform for development of this method, we first present an idealized analytic model for the energetic cross sections for ionization and excitation. This model uses the modified

*This research was supported by AFOSR and AFRL.

†Mathematics Department, University of California at Los Angeles, Los Angeles, CA 90095-1555 USA. fbarekat@math.ucla.edu, caflisch@math.ucla.edu, byan@math.ucla.edu

‡AFRL

Mott cross section for the energetic cross section of ionization and an extension of this cross section for excitation. The energetic cross sections for deexcitation and recombination are then found through detailed balance.

Simulation for this model is performed by random sampling from all of the relevant kinetic processes. A direct simulation method suffers from two difficulties: First, there are a large number of kinetic processes (i.e., excitation and deexcitation between any two atomic levels) with widely varying rates. Fair representation of all of these processes can require very small time steps. Second, random fluctuations can exhaust the finite number of simulation particles in some state. In subsequent work, we plan to develop coarse-graining and a multi-scale simulation strategy to reduce the effect of these two computational bottlenecks.

The remainder of this paper is organized as follows: The formulation of the kinetic processes and their rates, along with some preliminaries, are presented in Section 2. The corresponding Boltzmann equations are formulated in Section 3, and the analogue of Boltzmann's H-theorem. An idealized choice for the energetic cross sections is described in Section 4. A Monte Carlo particle method for simulation using a particle representation for the electrons is presented in Section 5. Computational bottle-necks and acceleration techniques for removing them are presented in Section 6. Computational results from this simulation method are presented in Section 7 Finally, conclusions and future directions are discussed in Section 8.

2 Formulation

The plasma is assumed to consist of electrons, ions of unit charge and neutral atoms at various excitation levels. The atoms and ions are modeled as a continuum with uniform density; the electrons are modeled through a velocity or energy (and direction) distribution function, which is simulated using a discrete set of particles. Throughout this paper, temperature T will have units of energy so that the Boltzmann constant k will be omitted.

2.1 The Distribution Function

The problems solved here will be spatially homogeneous and velocity isotropic. The distribution function is $f = f(E,t)$ with energy E. The equilibrium electron distribution is the (isotropic) Maxwell-Boltzmann distribution

$$f^{eq}(E) = n_e 2(\pi T_e^3)^{-1/2}\sqrt{E}e^{-E/T_e} \tag{1}$$

in which n_e is the number density of electrons and T_e is the electron temperature, so that

$$\begin{aligned}\int_0^\infty f^{eq}(E)\,\mathrm{d}E &= n_e\\ \int_0^\infty Ef^{eq}(E)\,\mathrm{d}E &= (3/2)n_eT_e.\end{aligned} \tag{2}$$

Similarly, the equilibrium densities ρ_k^{eq} for atoms at excitation level k with $k = 1,\ldots,k_{max}$ and ρ_{ion}^{eq} for ions are the Boltzmann and Saha distributions [5], respectively, given by

$$\rho_k^{eq} = c_a\rho_a g_k e^{-L_k/T_e}, \tag{3}$$

$$\rho_{ion}^{eq} = c_{ion}e^{-L_{ion}/2T_e}. \tag{4}$$

Note that in equilibrium, the ions and atoms have the same temperature as the electrons. Here L_k is the energy for kth excitation level, L_{ion} is the ionization energy and g_k is the degeneracy of level

k. The factor of 2 in the exponent in (4) is because ionization of one atom produces two particles: an ion and an electron. Note that by charge neutrality, $n_e = \rho_{ion}^{eq}$ in equilibrium.

As a simple model, use the values from the Bohr model

$$\begin{aligned} L_k &= (1 - k^{-2})I_H, \\ L_{ion} &= I_H, \\ g_k &= 2k^2, \end{aligned} \tag{5}$$

where I_H is the Rydberg unit of energy (13.6eV). The constant c_a is determined by normalization and c_{ion} comes from the Saha distribution [5] as

$$\begin{aligned} c_a &= \left(\sum_{k=1}^{k_{\max}} g_k e^{-L_k/T_e} \right)^{-1}, \\ c_{ion} &= \left(2 c_a \rho_a \lambda_e^{-3} \right)^{1/2}, \end{aligned} \tag{6}$$

in which $\lambda_e = h(2\pi m_e T_e)^{-1/2}$. In addition, define the binding energy B_k for level k and the velocity in terms of energy as

$$B_k = L_{ion} - L_k \tag{7}$$

$$\Delta E_{lu} = B_l - B_u. \tag{8}$$

$$v(E) = c_v \sqrt{E} = \sqrt{2E/m_e}. \tag{9}$$

2.2 Interaction Rates

Simulation of plasma kinetics is performed by a sequence of interactions among the components (atoms, ions and electrons) that are randomly chosen with the correct rates. Each interaction involves a choice of one or more electron energies; the atoms and ions are all assumed to be stationary because of their large relative mass. We assume that the differential cross section is angular independent. The energetic cross sections are denoted as

$$\begin{aligned} &\sigma_{ex}((l, E_0) \to (u, E_1)), \\ &\sigma_{de}((u, E_1) \to (l, E_0)), \\ &\sigma_{ion}((k, E_0, E_t) \to (E_1, E_2)), \\ &\sigma_{rec}((E_1, E_2) \to (k, E_0)), \end{aligned}$$

in which ionization, recombination, excitation and deexcitation are designated by the subscripts ion, rec, ex and de. For ionization and excitation, the energies, excitation level and angles are

$$\begin{aligned} E_0 &= \text{energy of incident electron} \\ E_1 &= E_0 - E_t = \text{energy of scattered electron} \\ E_2 &= E_t - B_k = \text{energy of ejected electron (for ionization)} \\ E_t &= \text{energy transferred from incident electron } (E_t = \Delta E_{lu} \text{ for excitation}) \\ l, k &= \text{atomic excitation level before ionization or excitation} \\ u &= \text{final atomic excitation level (for excitation)} \end{aligned} \tag{10}$$

while for recombination and deexcitationthe interaction is just reversed; i.e., E_1 and E_2 are the energies of incident electrons, E_0 is the energy of the final electron, and k or l is the level of the atom after recombination or deexcitation, and u is the level of the atom before deexcitation. Note the requirement that $E_0 > \Delta E_{lu}$ for excitation and that $E_0 > B_k$ for ionization.

The total rates R_{ion}, R_{rec}, R_{ex} and R_{de} for ionization, recombination, excitation and deexcitation (in units of #/(volume $\cdot$ time)) are

$$\begin{aligned}
R_{ion} &= \sum_k \rho_k \int_{B_k}^{\infty} \int_{B_k}^{E_0} v_0 \sigma_{ion}((k, E_0, E_t) \to (E_1, E_2)) f(E_0)\, \mathrm{d}E_t\, \mathrm{d}E_0, \\
R_{rec} &= \rho_{ion} \sum_k \int_0^{\infty} \int_0^{\infty} v_1 v_2 \sigma_{rec}((E_1, E_2) \to (k, E_0)) f(E_1) f(E_2)\, \mathrm{d}E_1\, \mathrm{d}E_2, \\
R_{ex} &= \sum_l \sum_{u>l} \rho_l \int_{\Delta E_{lu}}^{\infty} v_0 \sigma_{ex}((l, E_0) \to (u, E_1)) f(E_0)\, \mathrm{d}E_0, \\
R_{de} &= \sum_u \sum_{l<u} \rho_u \int_0^{\infty} v_1 \sigma_{de}((u, E_1) \to (l, E_0)) f(E_1)\, \mathrm{d}E_1.
\end{aligned} \tag{11}$$

It is convenient to define the rates r per electron (more precisely, per electron pair for recombination) as

$$\begin{aligned}
r_{ion}(k, E_0, E_t) &= \rho_k v(E_0) \sigma_{ion}((k, E_0, E_t) \to (E_1, E_2)) \\
r_{rec}(k, E_1, E_2) &= \rho_{ion} v(E_1) v(E_2), \sigma_{rec}((E_1, E_2) \to (k, E_0)), \\
r_{ex}(l, u, E_0) &= \rho_l v(E_0) \sigma_{ex}((l, E_0) \to (u, E_1)), \\
r_{de}(u, l, E_1) &= \rho_u v(E_1) \sigma_{de}((u, E_1) \to (l, E_0)),
\end{aligned} \tag{12}$$

and an integrated ionization rate per electron

$$r_{ion}^{tot}(k, E_0) = \int_{B_k}^{E_0} r_{ion}(k, E_0, E_t)\, \mathrm{d}E_t = \rho_k v(E_0) \sigma_{ion}^{tot}(k, E_0) \tag{13}$$

for which the cross section σ_{ion}^{tot} is defined in Section 4.1.

It follows that the detailed balance principle can be phrased as separate requirements for the energetic cross sections:

$$\rho_k^{eq} f_0^{eq} v_0 \sigma_{ion} = \rho_{ion}^{eq} f_1^{eq} f_2^{eq} v_1 v_2 \sigma_{rec}, \tag{14}$$

$$\rho_l^{eq} f_0^{eq} v_0 \sigma_{ex} = \rho_u^{eq} f_1^{eq} v_1 \sigma_{de}, \tag{15}$$

in which $f_i^{eq} = f^{eq}(E_i)$, $v_i = v(E_i)$ and in which

$$\begin{aligned}
\sigma_{ion} &= \sigma_{ion}((k, E_0, E_t) \to (E_1, E_2)), \\
\sigma_{rec} &= \sigma_{rec}((E_1, E_2) \to (k, E_0)), \\
\sigma_{ex} &= \sigma_{ex}((l, E_0) \to (u, E_1)), \\
\sigma_{de} &= \sigma_{de}((u, E_1) \to (l, E_0)).
\end{aligned}$$

3 The Boltzmann Equation and the H-Theorem

We formulate the Boltzmann equation and derive the H-Theorem in this section.

3.1 Boltzmann Equation

The Boltzmann equations for ionization/recombination and excitation/deexcitation are

$$\begin{aligned}
\partial_t f(E) &= Q_{IR}^e + Q_{ED}^e, \\
\partial_t \rho_k &= Q_{IR}^k + Q_{ED}^k, \\
\partial_t \rho_{ion} &= Q_{IR}^i,
\end{aligned} \tag{16}$$

in which the collision operators Q are defined below.

The H function is

$$H = \int f \log \frac{f}{f^{eq}} \,\mathrm{d}E + \sum_k \left(\rho_k \log \frac{\rho_k}{\rho_k^{eq}} + \rho_k - \rho_k^{eq} \right) + \rho_{ion} \log \frac{\rho_{ion}}{\rho_{ion}^{eq}}, \tag{17}$$

where f^{eq}, ρ_k and ρ_{ion} are the equilibrium values determined by the total number density and the total energy, see the appendix for details.

In the analysis below, we show that

$$\partial_t H \leq 0, \tag{18}$$

with equality if and only if $f(E)$, ρ_k and ρ_{ion} are the equilibrium values.

3.2 Ionization and recombination

The kinetic equations for ionization/recombination are

$$\begin{aligned}
\partial_t f(E) = Q_{IR}^e = & \sum_k \Big\{ \int \mathrm{d}E_t \rho_k f(E_0)(v_0 \sigma_i((k, E_0, E_t) \to (E_1 = E, E_2)) \\
& + \int \mathrm{d}E_0 \rho_k f(E_0)(v_0 \sigma_i((k, E_0, E_t) \to (E_1, E_2 = E)) \Big\} \\
& - \sum_k \Big\{ \int \mathrm{d}E_t \rho_{ion} f(E) f(E_2) v v_2 \sigma_r((E_1 = E, E_2) \to (k, E_0, E_t)) \\
& + \int \mathrm{d}E_0 \rho_{ion} f(E) f(E_1) v v_1 \sigma_r((E_1, E_2 = E) \to (k, E_0, E_t)) \Big\} \\
& + \sum_k \int \mathrm{d}E_t \rho_{ion} f(E_1) f(E_2) v_1 v_2 \sigma_r((E_1, E_2) \to (k, E_0 = E, E_t)) \\
& - \sum_k \int \mathrm{d}E_t \rho_k f(E) v \sigma_i((k, E_0 = E, E_t) \to (E_1, E_2)) \\
= & \sum_k \iint (\delta_1 + \delta_2 - \delta_0) \left(\rho_k f_0 v_0 \sigma_i - \rho_{ion} f_1 f_2 v_1 v_2 \sigma_r \right) \mathrm{d}E_0 \,\mathrm{d}E_t
\end{aligned} \tag{19}$$

$$\begin{aligned}
\partial_t \rho_k = Q_{IR}^k = & \iint \mathrm{d}E_t \,\mathrm{d}E_0 \rho_{ion} f(E_1) f(E_2) v_1 v_2 \sigma_r((E_1, E_2) \to (k, E_0, E_t)) \\
& - \iint \mathrm{d}E_t \,\mathrm{d}E_0 \rho_k f(E_0) v_0 \sigma_i((k, E_0, E_t) \to (E_1, E_2)) \\
= & - \iint \left(\rho_k f_0 v_0 \sigma_i - \rho_{ion} f_1 f_2 v_1 v_2 \sigma_r \right) \mathrm{d}E_0 \,\mathrm{d}E_t
\end{aligned} \tag{20}$$

$$\begin{aligned}
\partial_t \rho_{ion} = Q_{IR}^i = \partial_t \int f(E) \,\mathrm{d}E = & - \sum_k \partial_t \rho_k \\
= & \sum_k \iint \mathrm{d}E_t \,\mathrm{d}E_0 (\rho_k f_0 v_0 \sigma_i - \rho_{ion} f_1 f_2 v_1 v_2 \sigma_r)
\end{aligned} \tag{21}$$

in which

$$\begin{aligned}
E_1 &= E_0 - E_t, \\
E_2 &= E_t - B_k = E_t - (L_{\text{ion}} - L_k),
\end{aligned} \tag{22}$$

and

$$\delta_k = \delta(E - E_k).$$

We have used the short notation

$$\sigma_i = \sigma_i((k, E_0, E_t) \to (E_1, E_2)),$$
$$\sigma_r = \sigma_r((E_1, E_2) \to (k, E_0, E_t)).$$

Note that

$$\begin{aligned} \mathrm{d}E_1\,\mathrm{d}E_t &= \begin{vmatrix} \partial E_1/\partial E_0 & \partial E_1/\partial E_t \\ \partial E_t/\partial E_0 & \partial E_t/\partial E_t \end{vmatrix} \mathrm{d}E_0\,\mathrm{d}E_t = \begin{vmatrix} 1 & -1 \\ 0 & 1 \end{vmatrix} \mathrm{d}E_0\,\mathrm{d}E_t = \mathrm{d}E_0\,\mathrm{d}E_t, \\ \mathrm{d}E_0\,\mathrm{d}E_2 &= \begin{vmatrix} \partial E_0/\partial E_0 & \partial E_0/\partial E_t \\ \partial E_2/\partial E_0 & \partial E_2/\partial E_t \end{vmatrix} \mathrm{d}E_0\,\mathrm{d}E_t = \begin{vmatrix} 1 & 0 \\ 0 & 1 \end{vmatrix} DE_0\,\mathrm{d}E_t = \mathrm{d}E_0\,\mathrm{d}E_t, \end{aligned} \tag{23}$$

we can write down a compact weak form of (19)

$$\begin{aligned} \partial_t \iint \phi f\,\mathrm{d}E &= \iint \phi Q^e_{IR}\,\mathrm{d}E \\ &= \sum_k \iint (\phi_1 + \phi_2 - \phi_0)\left(\rho_k f_0 v_0 \sigma_i - \rho_{ion} f_1 f_2 v_1 v_2 \sigma_r\right)\,\mathrm{d}E_0\,\mathrm{d}E_t \\ &= \sum_k \iint (\phi_1 + \phi_2 - \phi_0)\left(\frac{\rho_k}{\rho_k^{eq}}\frac{f_0}{f_0^{eq}} - \frac{\rho_{ion}}{\rho_{ion}^{eq}}\frac{f_1}{f_1^{eq}}\frac{f_2}{f_2^{eq}}\right)\rho_k^{eq} f_0^{eq} v_0 \sigma_i\,\mathrm{d}E_0\,\mathrm{d}E_t, \end{aligned} \tag{24}$$

where we have used the formula (14) resulting from detailed balanced principle.

Similarly we have

$$\begin{aligned} \partial_t \rho_k &= Q^k_{IR} \\ &= -\iint \left(\rho_k f_0 v_0 \sigma_i - \rho_{ion} f_1 f_2 v_1 v_2 \sigma_r\right)\,\mathrm{d}E_0\,\mathrm{d}E_t \\ &= -\iint \left(\frac{\rho_k}{\rho_k^{eq}}\frac{f_0}{f_0^{eq}} - \frac{\rho_{ion}}{\rho_{ion}^{eq}}\frac{f_1}{f_1^{eq}}\frac{f_2}{f_2^{eq}}\right)\rho_k^{eq} f_0^{eq} v_0 \sigma_i\,\mathrm{d}E_0\,\mathrm{d}E_t. \end{aligned} \tag{25}$$

$$\begin{aligned} \partial_t \rho_{ion} &= Q^i_{IR} = -\sum_k Q^k_{IR} \\ &= \sum_k \iint \left(\frac{\rho_k}{\rho_k^{eq}}\frac{f_0}{f_0^{eq}} - \frac{\rho_{ion}}{\rho_{ion}^{eq}}\frac{f_1}{f_1^{eq}}\frac{f_2}{f_2^{eq}}\right)\rho_k^{eq} f_0^{eq} v_0 \sigma_i\,\mathrm{d}E_0\,\mathrm{d}E_t. \end{aligned} \tag{26}$$

We can derive the H-theorem.

Theorem 3.1. *For the entropy defined by (17), one has $H \geq 0$ and*

$$\partial_t H \leq 0$$

under the ionization/recombination kinetic equations (19)-(21). The equality holds if and only if $f(E)$, ρ_k and ρ_{ion} are the equilibrium values.

Proof. With the inequality $y \log \frac{y}{x} \geq (y - x)$, for $x, y > 0$, one has

$$H \geq \left(\int f\,\mathrm{d}E + 2\sum_k \rho_k + \rho_{ion}\right) - \left(\int f^{eq}\,\mathrm{d}E + 2\sum_k \rho_k^{eq} + \rho_{ion}^{eq}\right) = 0.$$

Here we have used the conserved quantity

$$n_{tot} = \int f\,\mathrm{d}E + 2\sum_k \rho_k + \rho_{ion}.$$

A straightforward computation gives

$$\begin{aligned}\partial_t H &= \int \partial_t f \log \frac{f}{f^{eq}}\,\mathrm{d}E + \sum_k \partial_t \rho_k \log \frac{\rho_k}{\rho_k^{eq}} + \partial_t \rho_{ion} \log \frac{\rho_{ion}}{\rho_{ion}^{eq}} + \partial_t n_{tot} \\ &= -\sum_k \iint \left(\log\left(\frac{\rho_k}{\rho_k^{eq}}\frac{f_0}{f_0^{eq}}\right) - \log\left(\frac{\rho_{ion}}{\rho_{ion}^{eq}}\frac{f_1}{f_1^{eq}}\frac{f_2}{f_2^{eq}}\right)\right)\left(\frac{\rho_k}{\rho_k^{eq}}\frac{f_0}{f_0^{eq}} - \frac{\rho_{ion}}{\rho_{ion}^{eq}}\frac{f_1}{f_1^{eq}}\frac{f_2}{f_2^{eq}}\right)\rho_k^{eq} f_0^{eq} v_0 \sigma_i \,\mathrm{d}E_0\,\mathrm{d}E_t \\ &\le 0.\end{aligned}$$

The equality holds if and only if

$$\frac{\rho_k}{\rho_k^{eq}}\frac{f_0}{f_0^{eq}} = \frac{\rho_{ion}}{\rho_{ion}^{eq}}\frac{f_1}{f_1^{eq}}\frac{f_2}{f_2^{eq}}, \tag{27}$$

for every E_0 and E_t.

One can show that this means

$$f = f^{eq}, \qquad \rho_k = \rho_k^{eq}, \qquad \rho_{ion} = \rho_{ion}^{eq}.$$

For completeness we give a proof in the appendix, with the assumption that f is smooth. □

3.3 Excitation/deexcitation

The kinetic equations for excitation/deexcitation are

$$\begin{aligned}\partial_t f(E) = Q_{ED}^e &= \sum_{k,\ell} \{ v' \sigma_e((k,E') \to (\ell,E))\rho_k f(E') \\ &\qquad - v\sigma_e((\ell,E) \to (k,E'))\rho_\ell f(E)\} \\ &= \sum_{l<u} \iint (\delta_1 - \delta_0)\left(\rho_l f_0 v_0 \sigma_e - \rho_u f_1 v_1 \sigma_d\right)\,\mathrm{d}E_0 \qquad (28) \\ \partial_t \rho_k = Q_{ED}^k &= \sum_\ell \int v\sigma_e((\ell,E) \to (k,E'))\rho_\ell f(E)\,\mathrm{d}E \\ &\qquad - \sum_\ell \int v'\sigma_e((k,E) \to (\ell,E'))\rho_k f(E')\,\mathrm{d}E' \\ &= \sum_{l<u} \iint \left(\rho_l f_0 v_0 \sigma_e - \rho_u f_1 v_1 \sigma_d\right)(\delta_{uk} - \delta_{lk})\,\mathrm{d}E_0 \qquad (29) \\ \partial_t \rho_{ion} = Q_{ED}^i &= 0 \qquad (30)\end{aligned}$$

in which $E' = E - \Delta E_{k\ell}$. To simplify notation, we write $\sigma_e((k,E) \to (\ell,E'))$ for both excitation (when $k < \ell$) and deexcitation (when $k > \ell$).

Again we have used the short notations

$$\begin{aligned}\sigma_e &= \sigma_e((l,E_0) \to (u,E_1)), \\ \sigma_d &= \sigma_d((u,E_1) \to (l,E_0)),\end{aligned}$$

where $E_1 = E_0 - \Delta E_{lu}$.

A compact weak form of (28) can be derived

$$\begin{aligned}\partial_t \iint \phi f\,\mathrm{d}E &= \iint \phi Q_{ED}^e\,\mathrm{d}E \\ &= \sum_{l<u} \iint (\phi_1 - \phi_0)\left(\rho_l f_0 v_0 \sigma_e - \rho_u f_1 v_1 \sigma_d\right)\,\mathrm{d}E_0 \\ &= \sum_{l<u} \iint (\phi_1 - \phi_0)\left(\frac{\rho_l}{\rho_l^{eq}}\frac{f_0}{f_0^{eq}} - \frac{\rho_u}{\rho_u^{eq}}\frac{f_1}{f_1^{eq}}\right)\rho_l^{eq} f_0^{eq} v_0 \sigma_e\,\mathrm{d}E_0,\end{aligned} \tag{31}$$

where we have used the formula (15) resulting from detailed balanced principle.

Similarly

$$\begin{aligned}\partial_t \rho_k &= Q_{ED}^k \\ &= \sum_{l<u} \iint \left(\rho_l f_0 v_0 \sigma_e - \rho_u f_1 v_1 \sigma_d\right)(\delta_{uk} - \delta_{lk})\,\mathrm{d}E_0 \\ &= \sum_{l<u} \iint \left(\frac{\rho_l}{\rho_l^{eq}}\frac{f_0}{f_0^{eq}} - \frac{\rho_u}{\rho_u^{eq}}\frac{f_1}{f_1^{eq}}\right)(\delta_{uk} - \delta_{lk})\rho_l^{eq} f_0^{eq} v_0 \sigma_e\,\mathrm{d}E_0.\end{aligned} \tag{32}$$

For excitation/deexcitation, the numbers of electrons, neutral atoms and do not change; i.e.,

$$\frac{\mathrm{d}}{\mathrm{d}t}\int f(E)\,\mathrm{d}E = \frac{\mathrm{d}}{\mathrm{d}t}\sum_k \rho_k = \frac{\mathrm{d}}{\mathrm{d}t}\rho_{ion} = 0.$$

We can derive a similar H-theorem. However the equilibrium is not unique and it depends on the distribution of initial data.

Theorem 3.2. *For the entropy defined by (17), one has $H \geq 0$ and*

$$\partial_t H \leq 0$$

under the excitation/deexcitation kinetic equations (28)-(30). The equality holds if

$$\frac{\rho_l}{\rho_l^{eq}}\frac{f_0}{f_0^{eq}} = \frac{\rho_u}{\rho_u^{eq}}\frac{f_1}{f_1^{eq}} \tag{33}$$

for every l, u and E_0.

The proof is similar as in the ionization/recombination case.

Note that with only excitation/deexcitation, the distributions f and ρ_k satisfying (33) are not necessary the equilibriums f^{eq} and ρ_k^{eq}. In fact, f is in the form

$$f(E) = f^{eq}(E)\phi(E), \tag{34}$$

where $\phi(E)$ is a periodic function with period ΔE such that ΔE_{lu} is an integer multiplication of ΔE, for every l, u. Note that ΔE_{lu} is a rational multiplication of I_H in our model, hence ΔE exists.

The derivation of $\phi(E)$ is given in the appendix. The dependence on the initial value implies that the equilibrium is not unique when the ionization/recombination process is absent. This is numerically studied in Section 7.4.

4 Idealized Energetic Cross Sections

4.1 Ionization

Ionization involves an incident electron with energy E_0 and two resulting electrons (one scattered, one emitted) with energies $E_1 = E_0 - E_t$ and $E_2 = E_t - B_k$ in which E_t is the transfer energy. Description of an ionization event then requires values of the energy transfer. Experimental measurements and numerical calculations of the resulting differential cross section have been performed (e.g., [1] or [4]) but the results are rather complicated. As an alternative, we use the semi-classical cross section [6]:

$$\sigma_{ion}((k, E_0, E_t) \to (E_1, E_2)) = 4\pi a_0^2 I_H^2 \frac{1}{E_0}\frac{1}{E_t^2}\mathbf{1}_{B_k \leq E_t \leq E_0}, \tag{35}$$

with a_0 the Bohr radius, I_H the Rydberg unit of energy.

For a fixed value of E_0, this formula for the cross section is symmetric with respect to E_1 and E_2, so that it is not possible to tell which of the resulting electrons was the scattered electron and which was the ejected electron.

The total cross section for a given choice of k and E_0 is $\sigma_{ion}^{tot}(k, E_0)$ given by

$$\begin{aligned}\sigma_{ion}^{tot}(k, E_0) &= \int_{B_k}^{E_0} \sigma_{ion}((k, E_0, E_t) \to (E_1, E_2))\, \mathrm{d}E_t \\ &= 4\pi a_0^2 I_H^2 \frac{1}{E_0}\left(\frac{1}{B_k} - \frac{1}{E_0}\right) \mathbf{1}_{E_0 > B_k}.\end{aligned} \tag{36}$$

The corresponding ionization rate per electron from (13) is

$$\begin{aligned}r_{ion}^{tot}(k, E_0) &= \rho_k v(E_0) \sigma_{ion}^{tot}(k, E_0) \\ &= 4\pi a_0^2 I_H^2 \sqrt{\frac{2}{m_e}} \frac{\rho_k}{\sqrt{E_0}}\left(\frac{1}{B_k} - \frac{1}{E_0}\right) \mathbf{1}_{E_0 > B_k}.\end{aligned} \tag{37}$$

In simulation of ionization from level k, the incident energy E_0 is chosen following (36), then the energy transfer E_t is chosen from the energy interval $B_k < E_t < E_0$ according to the probability density

$$p_{ion}(E_t) = \frac{\sigma_{ion}((k, E_0, E_t) \to (E_1, E_2))}{\sigma_{ion}^{tot}(k, E_0)} = \frac{1}{\frac{1}{B_k} - \frac{1}{E_0}} \frac{1}{E_t^2} \mathbf{1}_{B_k \le E_t \le E_0}. \tag{38}$$

4.2 Recombination

Recombination is a collision between an ion and two electrons of energy E_1 and E_2, one of which is absorbed into the atom, resulting in a scattered electron of energy E_0 and an atom at excitation level k. This interaction is determined by specification of E_1, E_2 and k. The principle of detailed balance (14) says that in equilibrium the processes of ionization and recombination must be in balance. As described in [5], the resulting Fowler relation says that

$$\sigma_{rec}((E_1, E_2) \to (k, E_0)) = \frac{g_k}{16\pi m_e h^{-3}} \frac{E_0}{E_1 E_2} \sigma_{ion}((k, E_0, E_t) \to (E_1, E_2)) \tag{39}$$

in which $E_1 = E_0 - E_t$ and $E_2 = E_t - B_k$. Note that the cross section is independent of temperature, as expected.

The corresponding recombination rate per pair of electrons from (12) is

$$\begin{aligned}r_{rec}(k, E_1, E_2) &= \rho_{ion} v(E_1) v(E_2) \sigma_{rec}((E_1, E_2) \to (k, E_0)) \\ &= \frac{2}{m_e} \frac{4\pi a_0^2 I_H^2}{16\pi m_e h^{-3}} \frac{\rho_{ion}}{\sqrt{E_1}\sqrt{E_2}} g_k \left(\frac{1}{(E_1 + B_k)^2} + \frac{1}{(E_2 + B_k)^2}\right).\end{aligned} \tag{40}$$

This rate is unbounded as $E_1 \to 0$ or $E_2 \to 0$.

4.3 Excitation

For the energetic cross section of excitation, we use the semi-classical cross section [6]

$$\sigma_{ex}((l, E_0) \to (u, E_1)) = (4\pi a_0^2 I_H^2)(3 f_{ul}) \frac{1}{E_0}\left(\frac{1}{\Delta E_{lu}} - \frac{1}{E_0}\right) \mathbf{1}_{E_0 > \Delta E_{lu}}, \tag{41}$$

where

$$f_{ul} = \frac{32}{3\pi\sqrt{3}} \frac{1}{l^5 u^3} \frac{1}{(l^{-2} - u^{-2})^3}$$

is the absorption oscillator strength,

$$\Delta E_{lu} = B_l - B_u$$

is the energy gap between the two levels l and u.

The corresponding excitation rate per electron from (12) is

$$r_{ex}(l,u,E_0) = (4\pi a_0^2 I_H^2)(3f_{ul})\sqrt{\frac{2}{m_e}}\frac{\rho_l}{\sqrt{E_0}}\left(\frac{1}{\Delta E_{lu}} - \frac{1}{E_0}\right)\mathbf{1}_{E_0>\Delta E_{lu}}. \tag{42}$$

4.4 Deexcitation

The principle of detailed balance (15) says that in equilibrium the processes of excitation and deexcitation must be in balance. As described in [5], the resulting Klein-Rosseland relation says that

$$\begin{aligned}\sigma_{de}((u,E_1)\to(l,E_0)) &= \frac{g_l}{g_u}\frac{E_0}{E_1}\sigma_{ex}((l,E_0)\to(u,E_1)) \\ &= (4\pi a_0^2 I_H^2)(3f_{ul})\frac{g_l}{g_u}\frac{1}{E_1}\left(\frac{1}{\Delta E_{lu}} - \frac{1}{E_1+\Delta E_{lu}}\right).\end{aligned} \tag{43}$$

The corresponding deexcitation rate per electron from (12) is

$$r_{de}(u,l,E_1) = (4\pi a_0^2 I_H^2)(3f_{ul})\sqrt{\frac{2}{m_e}}\rho_u\frac{g_l}{g_u}\frac{1}{\sqrt{E_1}}\left(\frac{1}{\Delta E_{lu}} - \frac{1}{E_1+\Delta E_{lu}}\right). \tag{44}$$

5 Monte Carlo Particle Method

Using the rates detailed in the previous sections, we now formulate a Monte Carlo simulation method for plasma dynamics, including ionization, recombination, excitation and deexcitation interactions between electrons and atoms/ions. The simulation is performed using a method like that of DSMC [3]. Coulomb collisions and other physical processes are not included here, but could be easily added to the method.

5.1 Particle/Continuum Representation

The plasma is described by a particle distribution for the electrons and a continuum description for the atoms and ions. The electron distribution function $f_e(E,\omega,t)$ is represented by the following discrete distribution

$$f_e(E,t) = m\sum_{j=1}^{N_e(t)}\delta(E-E_j(t))\delta(\omega-\omega_j(t)). \tag{45}$$

The number $N_e(t)$ of electrons is not constant because of ionization and recombination. The units of f are (number of particles) per energy per volume, and the constant m is the number of physical particles per numerical particle per volume.

The distribution of atoms is given by ρ_ℓ for atoms at excitation level ℓ for $1 \le \ell \le k_{max}$ and ρ_{ion} for ions. The atom density changes in response to the interactions with the electrons, and the energy and number of electrons is conserved, if one counts the number and binding energy of electrons in the atoms. There is a corresponding change in the ion density and electron density.

5.2 A no time counter DSMC method

Here we describe a Monte Carlo methods without time counter. The method contains two steps. First, the number of (virtual) collisions in each type is determined. Second, for each collision the involving particles are selected and updated.

Step 1. Decide the number of virtual collisions

First we want to find upper bounds of the numbers of collisions in each type. We need the upper bounds to be not too large, while at the same time easy to compute.

Denote $\tilde{N}$ the effective number, i.e., the number of physical particles represented by one numerical particle. The actual total rates of collisions in each type are

$$\begin{aligned}
\overline{r}_{ex} &= \tilde{N}\sum_{l<u}\sum_{k} r_{ex}(l,u,\varepsilon_k) \\
&= 12\pi a_0^2 I_H^2\sqrt{\frac{2}{m_e}}\tilde{N}\sum_{l}\sum_{u>l}\sum_{k}\frac{\rho_l}{\sqrt{\varepsilon_k}}f_{ul}\left(\frac{1}{\Delta E_{lu}}-\frac{1}{\varepsilon_k}\right)\mathbf{1}_{\varepsilon_k>\Delta E_{lu}} \\
\overline{r}_{de} &= \tilde{N}\sum_{u}\sum_{k} r_{de}(u,l,\varepsilon_k) \\
&= 12\pi a_0^2 I_H^2\sqrt{\frac{2}{m_e}}\tilde{N}\sum_{u}\sum_{l<u}\sum_{k}\frac{\rho_u g_l}{g_u}\frac{f_{ul}\sqrt{\varepsilon_k}}{\Delta E_{lu}(\Delta E_{lu}+\varepsilon_k)} \\
\overline{r}_{ion} &= \tilde{N}\sum_{l}\sum_{k} r_{ion}^{tot}(l,\varepsilon_k) \\
&= 4\pi a_0^2 I_H^2\sqrt{\frac{2}{m_e}}\tilde{N}\sum_{l}\sum_{k}\frac{\rho_l}{\sqrt{\varepsilon_k}}\left(\frac{1}{B_l}-\frac{1}{\varepsilon_k}\right)\mathbf{1}_{\varepsilon_k>B_l}
\end{aligned}$$

$$\begin{aligned}
\overline{r}_{rec} &= \tilde{N}^2\sum_{i<j}\sum_{l} r_{rec}(l,E_i,E_j) \\
&= \frac{4\pi a_0^2\rho_{ion}}{16\pi m_e h^{-3}}\frac{2}{m_e}I_H^2\tilde{N}^2\sum_{i<j}\frac{1}{\sqrt{E_iE_j}}\sum_{l} g_l\left(\frac{1}{(E_i+B_l)^2}+\frac{1}{(E_j+B_l)^2}\right) \\
&= \frac{4\pi a_0^2\rho_{ion}}{16\pi m_e h^{-3}}\frac{2}{m_e}I_H^2\tilde{N}^2\left(\sum_{i,j}\frac{1}{\sqrt{E_iE_j}}\sum_{l}\frac{g_l}{(E_i+B_l)^2}-\sum_{i}\frac{1}{E_i}\sum_{l}\frac{g_l}{(E_i+B_l)^2}\right) \\
&= \frac{4\pi a_0^2\rho_{ion}}{16\pi m_e h^{-3}}\frac{2}{m_e}I_H^2\tilde{N}^2\left(\sum_{j}\frac{1}{\sqrt{E_j}}\sum_{i}\left(\frac{1}{\sqrt{E_i}}\sum_{l}\frac{g_l}{(E_i+B_l)^2}\right)-\sum_{i}\frac{1}{E_i}\sum_{l}\frac{g_l}{(E_i+B_l)^2}\right)
\end{aligned}$$

Therefore we can take the upper bounds to be

$$\begin{aligned}
\tilde{r}_{ex} &= 12\pi a_0^2 I_H^2\sqrt{\frac{2}{m_e}}N_e\tilde{N}\sum_{l}\rho_l\sum_{u>l}\frac{2}{3\sqrt{3}}\frac{f_{ul}}{(\Delta E_{lu})^{3/2}} \\
\tilde{r}_{de} &= 12\pi a_0^2 I_H^2\sqrt{\frac{2}{m_e}}N_e\tilde{N}\sum_{u}\rho_u\sum_{l<u}\frac{g_l}{g_u}\frac{f_{ul}}{2(\Delta E_{lu})^{3/2}} \\
\tilde{r}_{ion} &= 4\pi a_0^2 I_H^2\sqrt{\frac{2}{m_e}}N_e\tilde{N}\sum_{l}\frac{2}{3\sqrt{3}}\frac{\rho_l}{(B_l)^{3/2}} \\
\tilde{r}_{rec} &= \frac{4\pi a_0^2\rho_{ion}}{16\pi m_e h^{-3}}\frac{2}{m_e}I_H^2\tilde{N}^2\sum_{j}\frac{1}{\sqrt{E_j}}\sum_{i}\left(\frac{1}{\sqrt{E_i}}\sum_{l}\frac{g_l}{(E_i+B_l)^2}\right)
\end{aligned}$$

Then

$$\tilde{R} = \tilde{r}_{ex}+\tilde{r}_{de}+\tilde{r}_{ion}+\tilde{r}_{rec}$$

is the total rate of all collisions. For a time step Δt, there are $\tilde{R}\Delta t$ virtual collisions performed. For the space homogeneous problem, one can take

$$\Delta t = \frac{1}{\tilde{R}},$$

such that exact one virtual collision happens in one time step. This eliminates the time error.

To evaluate $\tilde{R}$ one only needs the total computational cost of $O(L^2 + N_e)$ at beginning, with L the number of excitation levels. Besides, since only one or two electrons and one or two atom levels are updated after each collision, it's quite easy to update $\tilde{R}$.

Step 2. Perform one virtual collision

- 2.0 Decide the type of the virtual collision. The four types of collisions are selected with rates

$$\frac{\tilde{r}_j}{\tilde{R}}, \quad j \in \{ex, de, ion, rec\}.$$

For excitation,

- 2e.1 Pick up a free electron E_0 uniformly.
- 2e.2 Pick up a prior-collisional level l and post-collisional level $u > l$ with rate

$$\frac{\rho_l \frac{f_{ul}}{(\Delta E_{lu})^{3/2}}}{\sum_l \rho_l \sum_{u>l} \frac{f_{ul}}{(\Delta E_{lu})^{3/2}}}.$$

- 2e.3 If

$$rand \leq \frac{\frac{1}{\sqrt{E_0}} \left(\frac{1}{\Delta E_{lu}} - \frac{1}{E_0} \right) \mathbf{1}_{E_0 > \Delta E_{lu}}}{\frac{2}{3\sqrt{3}} \frac{1}{(\Delta E_{lu})^{3/2}}},$$

  accept the collision. Perform the excitation,

$$(l, E_0) \to (u, E_0 - \Delta E_{lu}).$$

  Otherwise reject it.

For deexcitation,

- 2d.1 Pick up a free electron E_0 uniformly.
- 2d.2 Pick up a prior-collisional level u and post-collisional level $l < u$ with rate

$$\frac{\rho_u \frac{g_l}{g_u} \frac{f_{ul}}{2(\Delta E_{lu})^{3/2}}}{\sum_u \rho_u \sum_{l<u} \frac{g_l}{g_u} \frac{f_{ul}}{2(\Delta E_{lu})^{3/2}}}.$$

- 2d.3 If

$$rand \leq \frac{\frac{\sqrt{E_0}}{\Delta E_{lu} + E_0}}{\frac{1}{2(\Delta E_{lu})^{1/2}}},$$

  accept the collision. Perform the deexcitation,

$$(u, E_0) \to (l, E_0 + \Delta E_{lu}).$$

  Otherwise reject it.

For ionization,

- 2i.1 Pick up a free electron E_0 uniformly.
- 2i.2 Pick up a prior-collisional level l with rate

$$\frac{\frac{\rho_l}{(B_l)^{3/2}}}{\sum_l \frac{\rho_l}{(B_l)^{3/2}}}.$$

- 2i.3 If

$$rand \leq \frac{\frac{1}{\sqrt{E_0}}\left(\frac{1}{B_l}-\frac{1}{E_0}\right)\mathbf{1}_{E_0>B_l}}{\frac{2}{3\sqrt{3}}\frac{1}{(B_l)^{3/2}}},$$

accept the collision. Sample the transferred energy E_t according to

$$\frac{1}{\frac{1}{B_l}-\frac{1}{E_0}}\frac{1}{E_t}$$

Perform the ionization,

$$(l, E_0) \to (E_0 - E_t, E_t - B_l).$$

Otherwise reject it.

The recombination,

- 2r.1 Pick up one free electron E_1 with rate

$$\frac{\frac{1}{\sqrt{E_j}}}{\sum_j \frac{1}{\sqrt{E_j}}},$$

and a second electron E_2 with rate

$$\frac{\frac{1}{\sqrt{E_i}}\sum_l \frac{g_l}{(E_i+B_l)^2}}{\sum_i\left(\frac{1}{\sqrt{E_i}}\sum_l \frac{g_l}{(E_i+B_l)^2}\right)}$$

This step can be accomplished by several different methods. In the numerical section part, we apply four different methods and compare their efficiencies.

- 2r.2 If the two electrons are the same one, reject the collision. Otherwise, pick up the post-collisional level l with rate

$$\frac{\frac{g_l}{(E_i+B_l)^2}}{\sum_l \frac{g_l}{(E_i+B_l)^2}}.$$

- 2r.3 Perform the recombination,

$$(E_1, E_2) \to (l, E_1 + E_2 + B_l).$$

6 Computational Bottlenecks and Acceleration Techniques

There are several difficulties in simulation of excitation/deexcitation and ionization/recombination: The rates for different interactions are widely varying, so that it is difficult to efficiently include all of the interactions. The recombination rate depends in a singular way on the electron energies, so that efficient and correct sampling of the electrons for recombination events is difficult. There may be too few atoms at a given level to accommodate the random choice of the number of interactions involving that level. For example, a difficulty occurs if m is larger than the atom or ion density ρ that is decreased in the collision.

The rates for transition between levels k and ℓ (with $k > \ell$) are of size $r_{k\ell} = \rho_k(B_\ell - B_k)^{-2}$. This is maximized for $\ell = k-1$. Since $\rho_k = O(g_k) = O(k^2)$ and $B_{k-1} - B_k = \left((1-(k-1)^{-2}) - (1-k^{-2})\right)^{-2} = O(k^6)$. It follows that $r_{kk-1} = O(k^8)$.

We have implemented several strategies to handle this rapid variation with k:

(1) The simplest strategy is to use a single value $\overline{r} = \sup \overline{r}^{k\ell}$ for the upper bound on the interaction rates (with separate treatment of recombination). Then for the virtual collisions, the values of (k, ℓ) can be chosen uniformly and the electron can be chosen uniformly from among the discrete set of electrons. Because of the wide range of interaction rates, this method is very inefficient.

(2) A direct method for choosing (k, ℓ) with the correct probability is performed by first creating a single index i for all pairs $(k, \ell) = (k(i), \ell(i))$ for $1 \le i \le (max + 1)^2$. For each virtual collision, choose a random number ξ and set $(k, \ell) = (k(j), \ell(j))$ in which j is the smallest integer so that

$$\sum_{i=1}^{j} \overline{R}(i) \ge \xi R_{max} \tag{46}$$

in which $\overline{R}(i) = \overline{R}(k(i), \ell(i))$. The choose the electron (or two electrons for recombination) uniformly from among the discrete set of electrons. This method is accurate, but somewhat inefficient because of the sum in (46).

(3)A more efficient method is to group together the interactions (k, ℓ) and (ℓ, k), and to sequential go through values of (k, ℓ) with $k < \ell$. For each value of (k, ℓ), there are $(\overline{R}(k, \ell) + \overline{R}(\ell, k))dt$ virtual interactions in the time interval dt. For each interaction, randomly choose the interaction (k, ℓ) with probability $p = \overline{R}(k, \ell)/(\overline{R}(k, \ell) + \overline{R}(\ell, k))$ or (ℓ, k) with probability $1-p$. This method is quite efficient for excitation, deexcitation and ionization, but does not solve the problems of inefficient sampling for recombination. Although there is no guarantee that this method is unbiased, we have seen no differences between its results and those of method (2). Note that sequentially going through values of (k, ℓ) without grouping (k, ℓ) and (ℓ, k) does not work unless the time step is very small.

(4) Coarse grain the excitation levels into "super-levels" containing a number of individual levels. Characterize each super level by a density and temperature for that super-level. Within each super-level, use the Maxwellian density (3) to give the density for each indivudal level.

7 Computational Results

This section presents computational results from the simulation method described above. All of the computations presented here are for an initial temperature of $T = 25000$ K and number density $n_{tot} = 10^{25}$ for all (free and bound) electrons. $100,000$ computational particles are used to represent the electron distribution function. The model for the neutral atoms consists of five levels.

7.1 Equilibrium initial data

The first results are for a distribution of electrons, neutral atoms and ions that in are the equilibrium distribution given by (1), (3) and (4). Figure 1 shows the electron energy distribution function at

various times. The plot on the top is for a simulation that includes excitation/deexcitation alone with no ionization/recombination; while that on the bottom is for ionization/recombination with no excitation/deexcitation. The fluctuations in the results are due to statistical fluctuations in the simulation due to a finite number of computational particles.

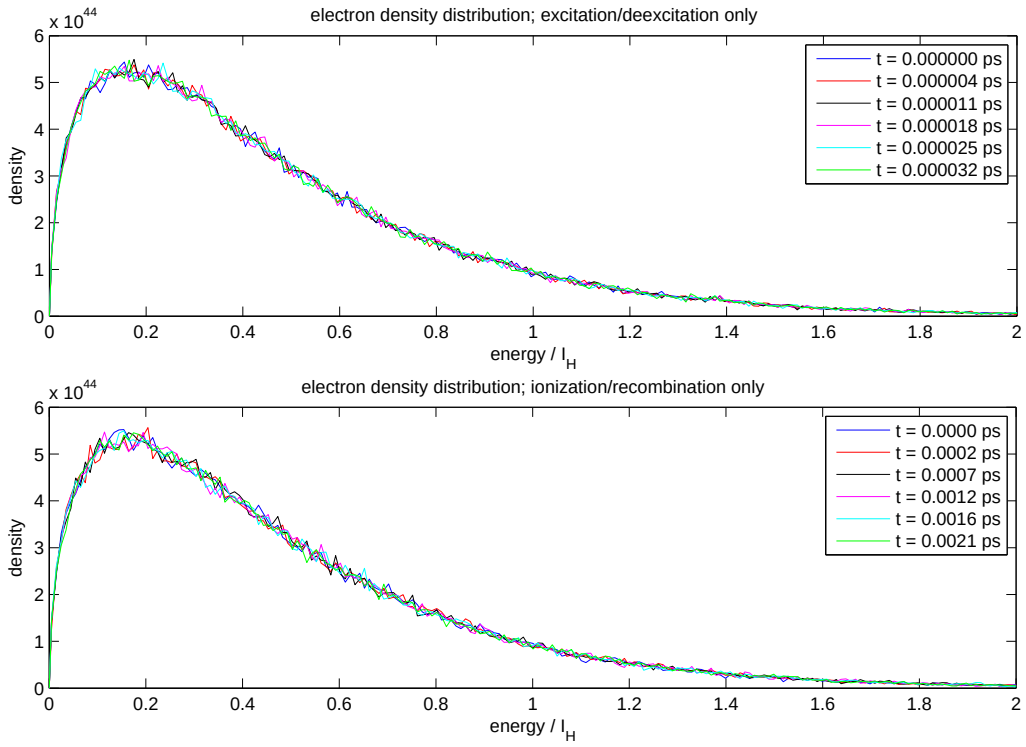

Figure 1: Electron density function at various times starting from equilibrium, with excitation/deexcitation only (top), and ionization/recombination only (bottom) These results show that the simulation method does preserve the equilibrium distribution as required. 100000 samples for free electrons.

7.2 Non-equilibrium initial data

The second simulation result, shown in Figure 2 - , is for initial data for which all of the neutral atoms are distributed at the ground level. The electrons and ions are initially in an equilibrium distribution given by (1) and (4).

In Figure 2, 3, 4, only excitation/deexcitation processes are included. The plots in the left column of Figure 2 show the density of the five different atomic levels (blue bars) at various times, demonstrating convergence to equilibrium (white bars) given by (3). The plots in the right column show the density distribution of free electrons (blue lines) at various times, demonstrating convergence to equilibrium (red dotted lines) given by (1).

Figure 3 shows the time evolution of entropy H, which is monotonically decreasing to its equilibrium value, except for fluctuations due to the finite number of sampled particles.

Figure 4 shows the time evolution of ratios of each type of virtual collisions (top), accepted collisions (middle) and acceptance rate (bottom). The acceptance rates of each virtual collision are above 50%, showing the high efficiency of our method.

Note that with only excitation/deexciation, the stationary state of electron distribution is different to the equilibrium by a periodic function ϕ, according to (34). However with 5 excitation levels

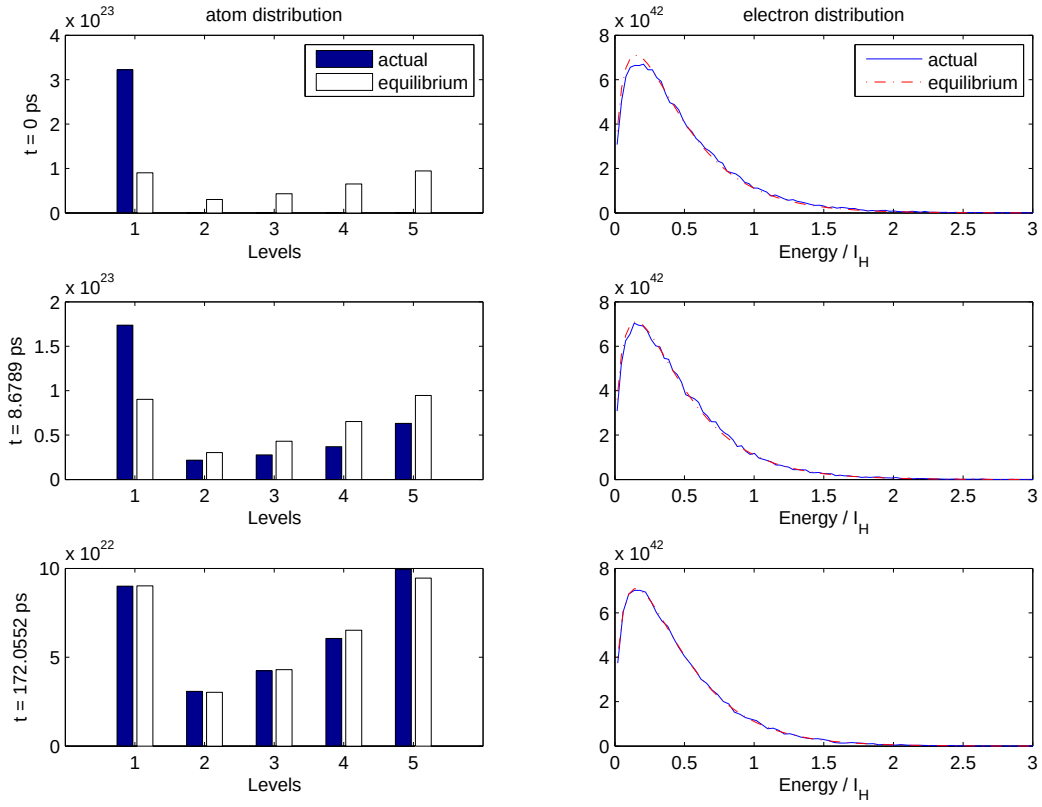

Figure 2: Snapshots of time evolution of atoms (left) and electron distributions (right), compared to the equilibrium (white bars and red dotted lines), starting from all neutral atoms at the ground level. Only excitation/deexcitation processes are included.

the period of ϕ is

$$\Delta E = \frac{1}{3^2 4^2 5^2} I_H = \frac{I_H}{3600},$$

which is too small to be observed in this experiment.

In Figure 5, 6, 7, similarly results are obtained with only ionization and recombination. In this case the stationary state of electron distribution is exactly the equilibrium.

7.3 Comparison of different methods on sampling electrons in recombination

In step 2r.1 we need to pick out an electron E_k with rate $\frac{v_k}{\sum_{k=1}^{N} v_k}$. Here $v_k = \frac{1}{\sqrt{E_k}}$ for the first electron, and $v_k = \frac{1}{\sqrt{E_k}} \sum_l \frac{g_l}{(E_k + B_l)^2}$ for the second electron.

We can apply four different methods.

7.3.1 Regular rejection method

For this method, we compute

$$v_{\max} = \max_{1 \le k \le N} v_k.$$

Then we uniformly pick up an electron E_k and accept it with rate $\frac{v_k}{v_{\max}}$. We keep sampling until one electron is accepted.

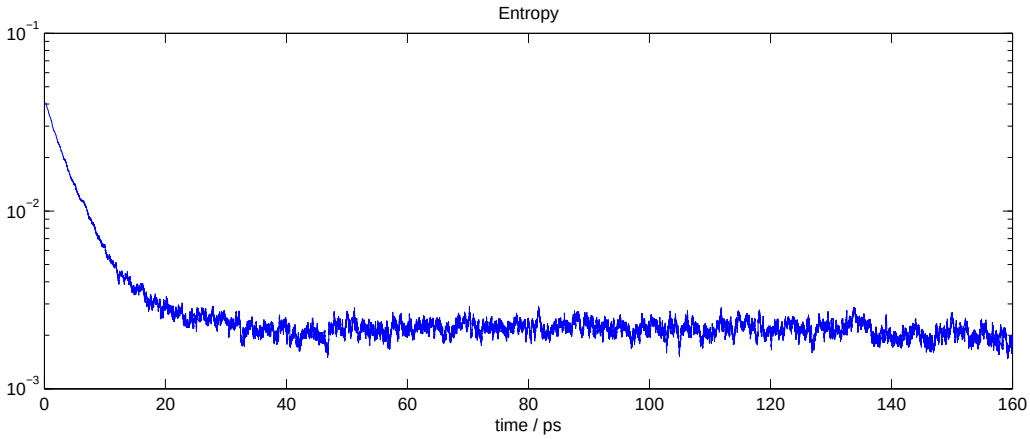

Figure 3: Time evolution of entropy, starting from all neutral atoms at the ground level. Only excitation/deexcitation processes are included.

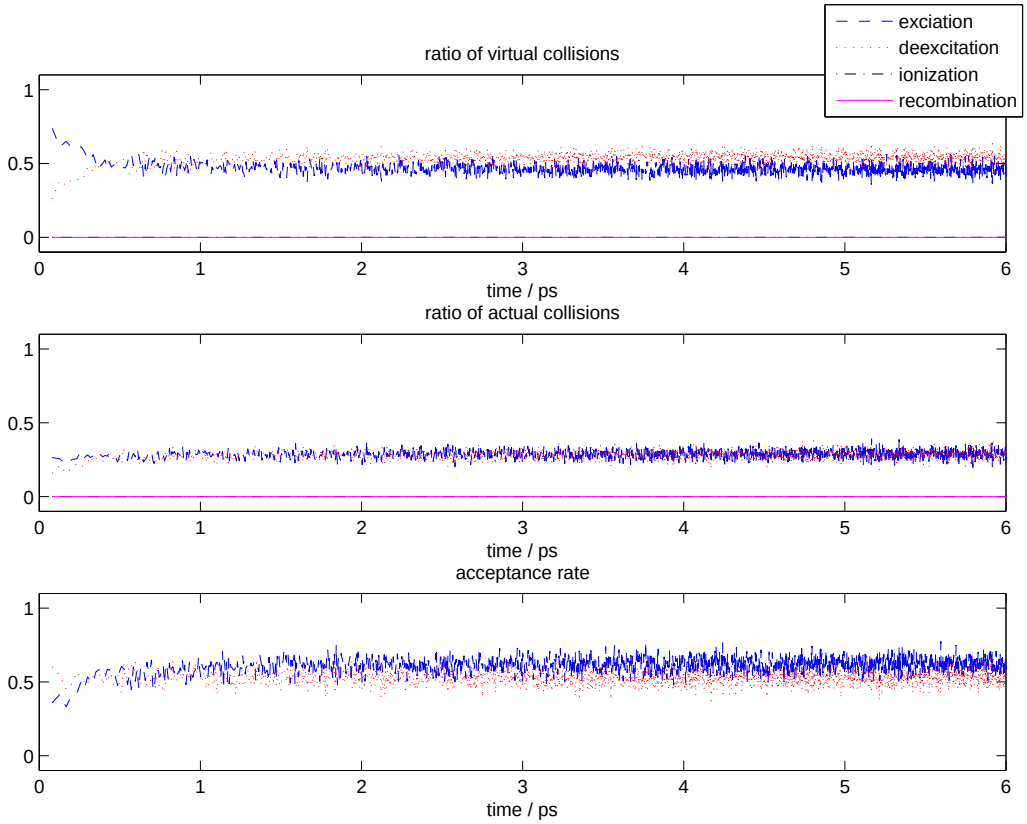

Figure 4: Time evolution of ratios of each type of virtual collisions (top), accepted collisions (middle) and acceptance rate (bottom), starting from all neutral atoms at the ground level. Only excitation/deexcitation processes are included.

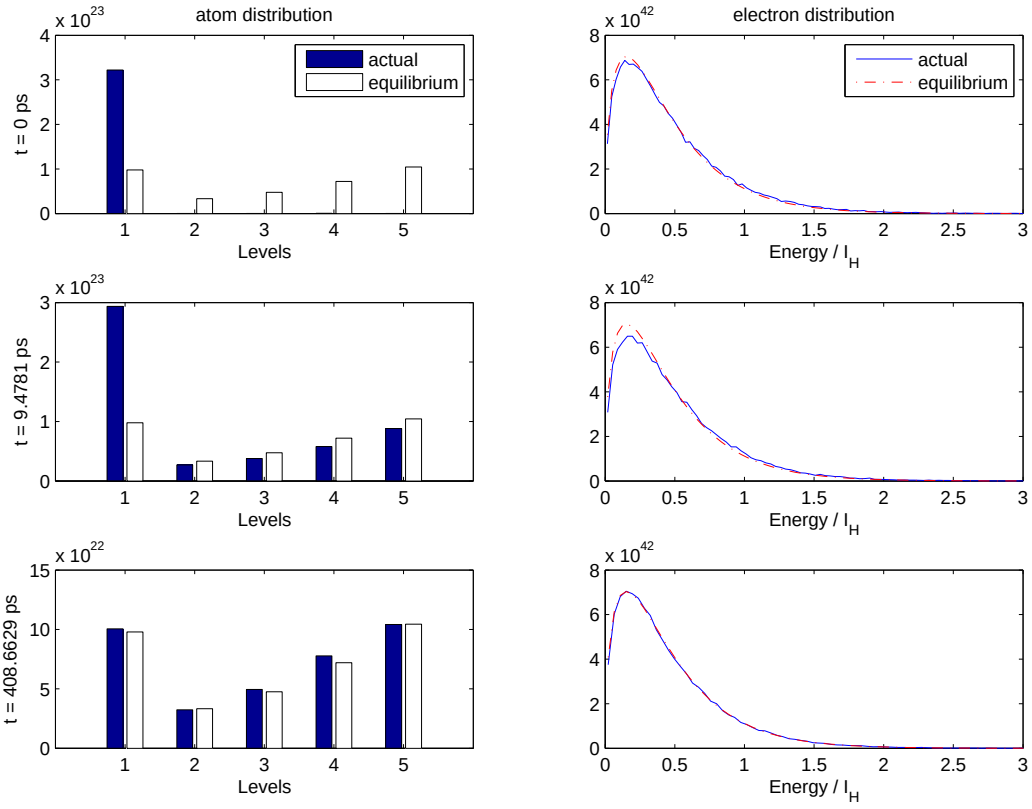

Figure 5: Snapshots of time evolution of atoms (left) and electron distributions (right), compared to the equilibrium (white bars and red dotted lines), starting from all neutral atoms at the ground level. Only ionization/recombination processes are included.

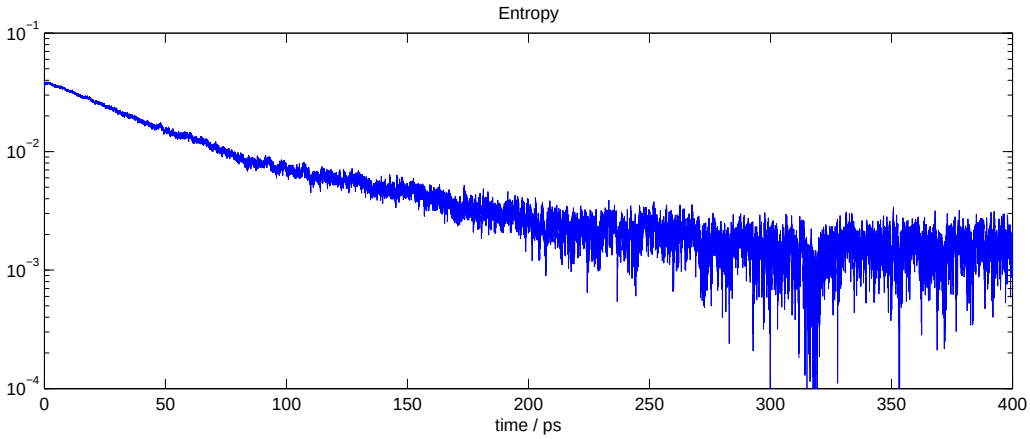

Figure 6: Time evolution of entropy, starting from all neutral atoms at the ground level. Only ionization/recombination processes are included.

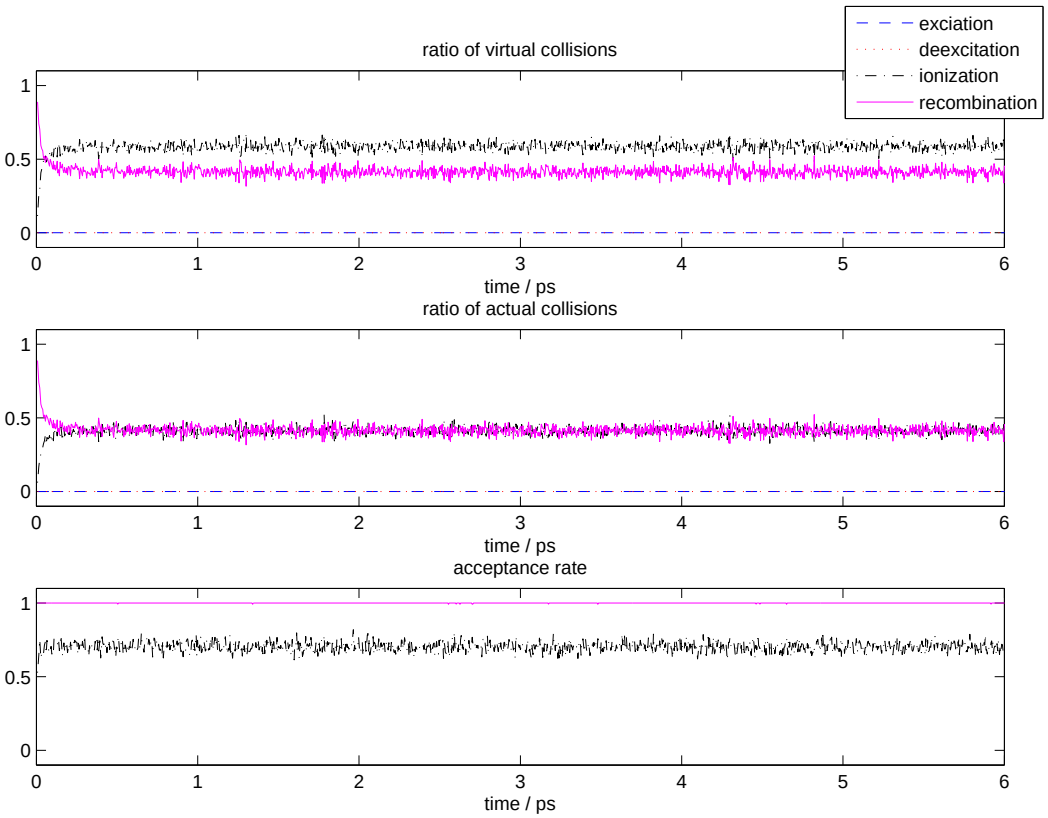

Figure 7: Time evolution of ratios of each type of virtual collisions (top), accepted collisions (middle) and acceptance rate (bottom), starting from all neutral atoms at the ground level. Only ionization/recombination processes are included.

The $v_{\max}$ can be pre-computed and updated after each collision.

This method is very inefficient due to the singularity as $E \to 0$. At equilibrium,

$$P(E < E_*) = C \int_0^{E_*} \sqrt{E} e^{-E/T_e} \, \mathrm{d}E = O(E_*^{3/2}).$$

Therefore

$$P\left(\min_{1 \le k \le N} E_k \le E_* \right) = 1 - (1 - P(E < E_*))^N = N E_*^{3/2}.$$

Hence the minimum of E is $O(N^{-2/3})$. The acceptance rate is

$$r_{regular} = \frac{1}{(\min_{1 \le k \le N} E_k)^{-1/2}} = O(N^{-1/3}).$$

Therefore the total cost to simulate to a fixed ending time is

$$C_{regular} = O\left(\frac{N}{r_{regular}} \right) = O(N^{4/3}).$$

7.3.2 Direct search method

A direct search method is to sample a number r from the uniform distribution over $(0, 1)$ and find

$$k = \min \left\{ j, \qquad s.t. \quad \sum_{i=1}^{j} v_i \ge r \sum_{i=1}^{N} v_i \right\}. \tag{47}$$

Here the summation $s = \sum_{k=1}^{N} v_k$ can be pre-computed and updated after each collision.

In this method the singularity is not a problem. However the searching for k needs $O(N)$ operations. The total cost to simulate to a fixed ending time is

$$C_{direct} = O(N^2).$$

7.3.3 Binary search method

We can accelerate the searching for k in (47). If we divide $[0, N]$ to two equal size subdivisions and first locate which division E_k is in, we only need $N/2$ operations to search in the corresponding subdivisions. If we apply this idea iteratively to each subdivision, the total cost can be reduced to $O(\log_2 N)$.

For this method we need to pre-compute and update the summation $s = \sum v_k$ in each subdivision. A total number of $O(\log_2 N)$ updates is need for each collision.

We give a detailed algorithm in the appendix.

The total cost to simulate to a fixed ending time is

$$C_{binary} = O(N \log_2 N).$$

7.3.4 Reduced rejection method

The reduced rejection method can be applied, by combining with the Marsaglia table, see [2].

There are two sources of computation costs. The Marsaglia table is re-created after K collisions, making the cost of sampling one electron to be $O(K^{1/3})$ when using regular acceptance/rejection

method in the L-region (see [2] for details). Hence the total cost is $O(NK^{1/3})$. The cost of re-creating one Marsaglia table is $O(N)$. The total cost in this part is $O\left(\frac{N}{K}N\right)$. Therefore the total cost of reduced rejection method is

$$C_{reducedrej} = O\left(NK^{1/3} + \frac{N^2}{K}\right) = O(N^{5/4}),$$

if we can take $K = N^{3/4}$.

In practice, we use a simple technique to make the two costs approximately equal:

- Step 1. Create the Marsaglia table. Record the computation time as t_{table}.
- Step 2. Perform collisions. Keep track of the total time t_{sample} used in sampling particles for recombination. When
$$t_{sample} > t_{table},$$
set $t_{sample} = 0$ and go to step 1.

7.3.5 The comparison

We apply these methods to the excitation/ionization problem and make a comparison.

The first test problem is the simulation of non equilibrium process. Initially all electrons are ionized and given by a Maxwellian. We take the total electron density $n_{tot} = 10^{28}$ and the temperature of free electron $T = 50,000$ K. In this case the ionization ratio at equilibrium is 38.04%. We simulate the decaying process until $t = 2 \times 10^{-3} ps$. At the end time, the ionization ratio is around 39.7%, indicating that the system is close to the equilibrium.

We solve this problem with numbers of samples to be

$$N = 12500, 25000, 50000, 100000, 200000, 400000, 800000$$

respectively for the initial free electrons. We track the time spent on the processes related to the sampling of electrons for recombination collisions. For reduced rejection method this includes the rebuilding of the Marsaglia tables and the sampling process. For the fast sampling method, this includes the updating of the summation tables and the sampling process. For direct sampling method, only the sampling process are timed.

The results are shown in Figure 8. As expected the direct search method needs $O(N^2)$ computations. It's getting extremely slow when more than 10^6 samples are used. The regular rejection method needs $O(N^{1.5})$ computation, which is slightly worse than expected. The cost of reduced rejection method is $O(N^{1.25})$, which coincides with the theoretical result. The cost for binary search method is $O(N^{1.1})$, which is close to the theoretical result $O(N \log N)$.

A similar test is applied on the simulation of equilibrium process. The system stays at equilibrium for all the time. Again we take the total electron density $n_{tot} = 10^{28}$ and the temperature of free electron $T = 50,000$ K. The ionization ratio stays around 38.04%. The simulation is perform until time $t = 10^{-4} ps$. The results are shown in Figure 9. We observe similar efficiencies as in the non-equilibrium test.

7.4 The stationary states without ionization/recombination

In the section we compute the stationary stats with only exciation/deexcitation processes. We include only two excitation levels. The period of the stationary function $\phi(E)$ in (34) is

$$\Delta E = \Delta E_{12} = L_2 - L_1 = \frac{3}{4} I_H.$$

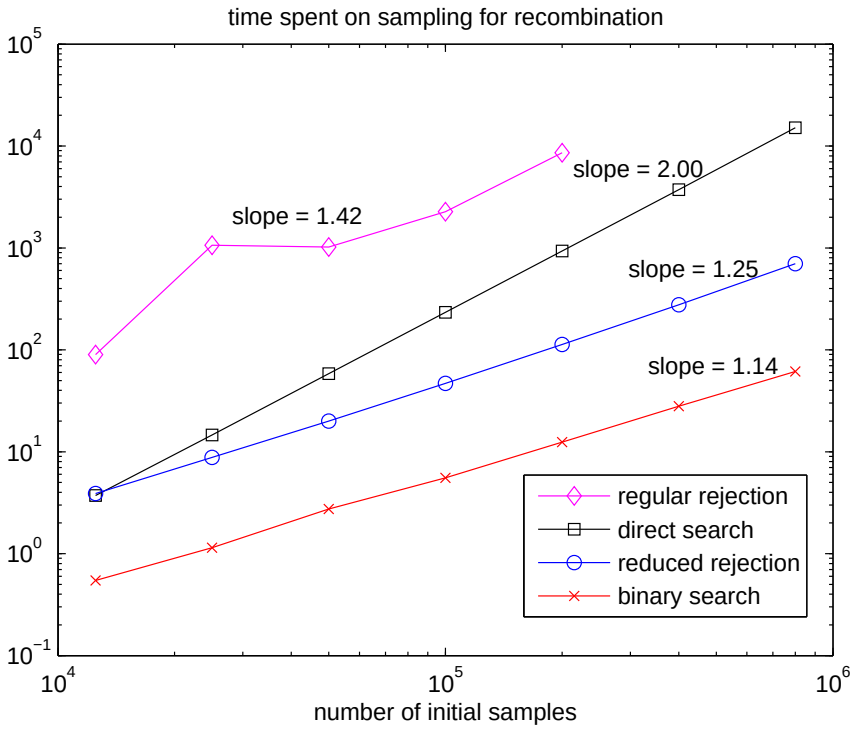

Figure 8: The time cost in the recombination collisions when various numbers of samples are used for the initial free electron distribution. Initially all atoms are ionized.

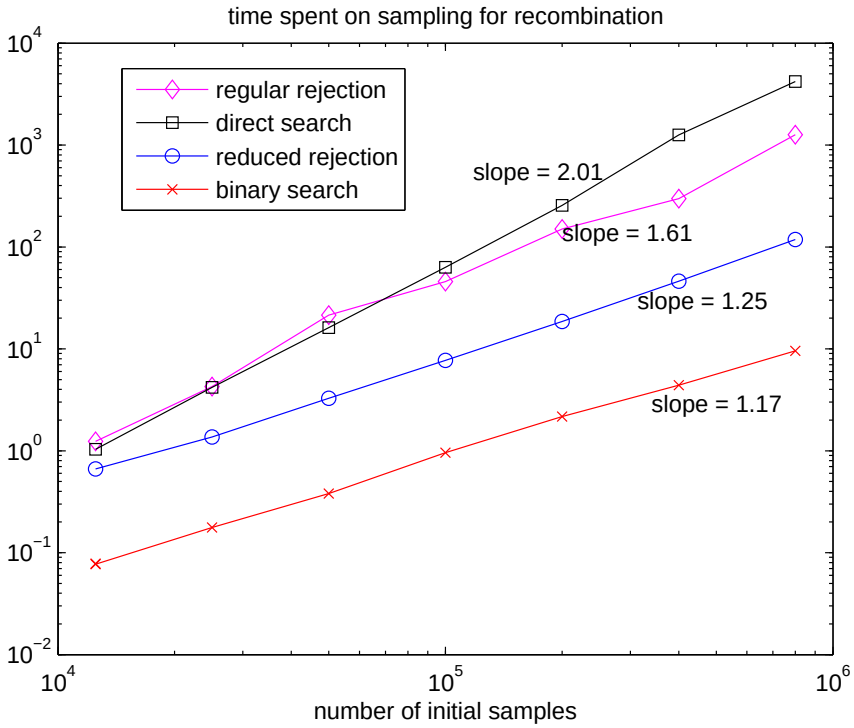

Figure 9: The time cost in the recombination collisions when various numbers of samples are used for the initial free electron distribution. The system stays in equilibrium for all the time.

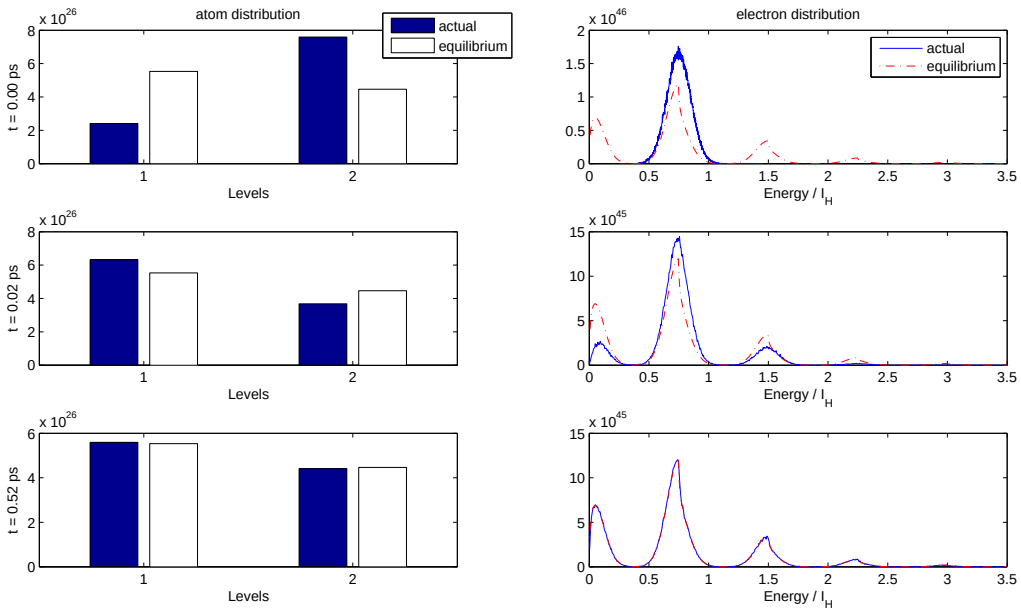

Figure 10: Snapshots of time evolution of atoms (left) and electron distributions (right), compared to the equilibrium (white bars and red dashed lines), starting from the initial data (48). Only excitation/deexcitation processes are included. 2×10^5 samples are used for free electrons.

Initially the free electrons concentrate near $E = \Delta E$

$$f(E,0) = \frac{n_e}{\sqrt{2\pi T_0}} e^{-\frac{(E-\Delta E)^2}{2T_0}}, \tag{48}$$

with $T_0 = \frac{1}{10}\Delta E$. Here we take $n_e = 10^{28}$.

The time evolution is shown in Figure 10. The stationary of the electron distribution clearly shows the period of $\frac{3}{4} I_H$.

Figure 10 shows the time evolution of the entropy

$$H = \frac{1}{n_{tot}} \left(\int f \log \frac{f}{f^{eq}\phi} \, \mathrm{d}E + \sum_k \left(\rho_k \log \frac{\rho_k}{\rho_k^{eq}} \right) \right),$$

where f^{eq} and ϕ are defined in Appendix C. This verifies the convergence to the theoretical result.

8 Conclusions

This paper presented an idealized model for excitation/deexcitation and ionization/recombination and a Monte Carlo method for its simulation. The energetic cross sections for the model are all given by analytic formulas and they are consistent with detailed balance. Moreover, there are sampling methods for each of the cross sections, using either direct sampling or reduced rejection method.

A direct simulation method for this model was formulated following the DSMC method, but it is extremely inefficient due to the wide range of rates for excitation/deexcitation. This computational obstacle has been removed by rearranging the events make the sampling more efficient. A second computational difficulty is that statistical fluctuations can lead to negative particle numbers by due to removal of more particles than are numerically realized. This difficulty can be prevented by

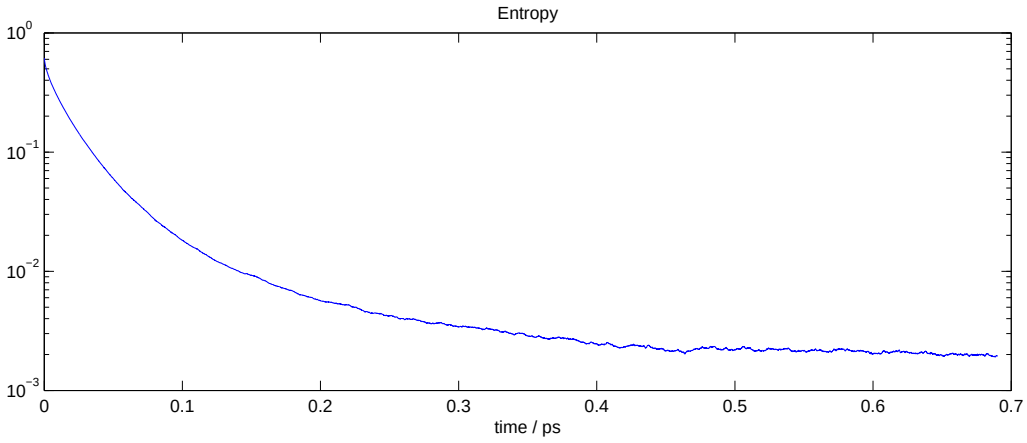

Figure 11: Time evolution of entropy, the initial data (48). Only excitation/deexcitation processes are included. 2×10^5 samples are used for free electrons.

taking small time steps, but that slows down the computation. A second remedy is coarse graining of the excitation levels. These acceleration methods will be the subject of a subsequent paper.

The model and method here has been developed under a number of simplifying assumptions: The energy levels come from the Bohr model of hydrogen; all ions have charge +1; Coulomb collisions have been neglected. Generalization to more realistic models can be easily performed.

9 Acknowledgments

References

[1] M. Baertschy, T.N. Rescigno, W.A. Isaacs, X. Li, and C.W. McCurdy. Electron-impact ionization of atomic hydrogen. *Phys. Rev. A*, 63:022712, 2001.

[2] Farzin Barekat and Russel Caflisch. Simulation with fluctuating and singular rates. *preprint*.

[3] G.A. Bird. *Molecular Gas Dynamics*. Oxford University Press, London, 1976.

[4] N.F. Mott and H.S.W. Massey. *The Theory of Atomic Collisions*. Oxford University Press, London, 1965.

[5] John T. Oxenius. *Kinetic Theory of Particles and Photons*. Springer-Verlag, Berlin, 1986.

[6] Y .B. Zel'dovich and Y. P. Raizer. *Physics of Shock Waves and High-Temperature Hydrodynamic Phenomena*. Dover Publications, Inc., New York, 2002.

A The equilibrium states in ionization/recombination collisions

Once the initial data given, the equilibrium states can be determined by the total number density of (free and bound) electrons n_{tot} and the total energy E_{tot}.

If the ionization and recombination processes are included, the number density of free electrons n_e varies with time. We need to determine n_e, as well as the temperature T_e, at equilibrium.

Due to the density and energy conservation, T_e satisfies

$$\frac{3}{2} n_e T_e + \sum_k \rho_k^{eq} L_k + \rho_{ion}^{eq} L_{ion} = E_{tot}, \tag{49}$$

where

$$\begin{aligned} n_e &= \rho_{ion}^{eq} = c_{ion} e^{-L_{ion}/T_e}, \\ \rho_k^{eq} &= (n_{tot} - n_e) c_a g_k e^{-L_k/T_e}, \end{aligned} \tag{50}$$

with c_a, c_{ion}, g_k, L_k, L_{ion} given in Section 2.1. Note that c_a and c_{ion} also depend on T_e.

One can easily solve out T_e by a Newton's method.

B Equilibrium in H theorem for ionization/recombination

In this appendix we show that formula (27) implies

$$f = f^{eq}, \qquad \rho_k = \rho_k^{eq}, \qquad \rho_{ion} = \rho_{ion}^{eq}.$$

Denote

$$C_k = \frac{\rho_k}{\rho_k^{eq}}, \qquad C_i = \frac{\rho_{ion}}{\rho_{ion}^{eq}}, \qquad h = \frac{f}{f^{eq}}.$$

Then

$$C_k h(E_0) = C_i h(E_0 - E_t) h(E_t - B_k),$$

for any k, E_0 E_t satisfying $B_k \le E_t \le E_0$.

Take the derivative with respect to E_t on both sides, one has

$$-h'(E_0 - E_t)h(E_t - B_k) + h(E_0 - E_t)h'(E_t - B_k) = 0,$$

$$\frac{h'(E_0 - E_t)}{h(E_0 - E_t)} = \frac{h'(E_t - B_k)}{h(E_t - B_k)}.$$

Denote $\phi = \log h$, then

$$\phi'(E_0 - E_t) = \phi'(E_t - B_k).$$

This formula is valid for any E_0, therefore ϕ' is a constant. h has the form

$$h = e^{\alpha E + \beta},$$

where both α and β are constants. Then

$$C_k = C_i e^{-\alpha B_k + \beta} = C_i e^{-\alpha L_{ion} + \beta} e^{\alpha L_k}.$$

This means that f, ρ_k and ρ_{ion} are at equilibrium with temperature

$$\left(\frac{1}{T_e} - \alpha \right)^{-1},$$

where T_e is the temperature of f^{eq}. Since the equilibrium temperature is unique due to the conservation of number density and energy, we have

$$\alpha = 0.$$

Then the conservation of number density gives $\beta = 0$. We have

$$h = 1, \qquad C_k = 1, \qquad C_i = 1.$$

C The stationary states in excitation/deexcitation collisions

In this appendix we show how to derive the stationary states (34) with only excitation/deexcitation included.

The solution of equation (33) is of the form

$$\begin{aligned} f(E) &= f^{eq}(E;T)\phi(E), \\ \rho_k &= \rho_k^{eq}(T), \end{aligned} \tag{51}$$

where the equilibrium temperature T and the periodic function $\phi(E)$ are to be determined below. The number density of the atom equilibrium is given by the initial data,

$$\rho_a = \sum_k \rho_k(t=0).$$

For any given E_0, we multiply the first equation in (51) by $\sum_{j=0}^{\infty}\delta(E-E_0-j\Delta E)$ and integrate over $\{E>0\}$, we obtain

$$\int \sum_j \delta(E-E_0-j\Delta E) f(E)\,\mathrm{d}E = \int \sum_j \delta(E-E_0-j\Delta E) f^{eq}(E)\phi(E)\,\mathrm{d}E$$
$$\sum_j f(E_0+j\Delta E) = \sum_j f^{eq}(E_0+j\Delta E)\phi(E_0).$$

Therefore,

$$\phi(E_0) = \frac{\sum_j f(E_0+j\Delta E)}{\sum_j f^{eq}(E_0+j\Delta E)} = \frac{\sum_j f(E_0+j\Delta E, t=0)}{\sum_j f^{eq}(E_0+j\Delta E)}. \tag{52}$$

Here we have used the equation

$$\frac{\mathrm{d}}{\mathrm{d}t}\sum_j f(E+j\Delta E,t) = 0,$$

due to the fact that an electron can only gain or lose an energy of integer multiplication of ΔE with only excitation/deexcitation included.

We still need to find out the equilibrium temperature T, which can be solved from the energy conservation

$$\int E f^{eq}(E;T)\phi(E)\,\mathrm{d}E + \sum_k \rho_k^{eq}(T)L_k + n_e L_{ion} = E_{tot}.$$

Again the Newton's method can be applied.

D Algorithm for binary search method

In this appendix we give the detailed algorithm for binary search method

D.1 Padding zeros

For a given set $\{v_k, k=1,\ldots,N\}$, we first enlarge its size to N_1 by padding zeros. Here N_1 is the minimum power of 2 satisfying $N_1 \geq N$. In the following we assume N is a power of 2 and $N_1 = N$, without loss of generality.

D.2 Building a table

Let $L = \log_2 N$. We need to build a table to store the pre-computed summations,

$$s_{l,j} = \sum_{i=(j-1)2^{L-l}+1}^{j2^{L-l}} v_i, \quad \text{with } 0 \le l \le L, 1 \le j \le 2^l.$$

Noting that

$$s_{L,j} = v_j,$$

we don't need to store $s_{L,j}$, for the purpose of saving memory.

The total memory used for storing this table is

$$1 + 2 + \cdots + 2^{L-1} = 2^L - 1 = N - 1.$$

Beside, the table $\{s_{l,j}\}$ can be computed backwardly

$$s_{l,j} = s_{l+1,2j-1} + s_{l+1,2j}.$$

Hence we only need to carry out N summations.

D.3 Sampling a particle

Here we describe the algorithm for sampling.

Sample r uniformly from $(0, 1)$
Let $k = 1$, $q = s_{0,1} = \sum_j v_j$
for $l = 1, \ldots, L$ **do**
  $q_1 \leftarrow s_{l,2k-1}$
  $p \leftarrow \frac{q_1}{q}$
  if $r \le p$ **then**
    $k \leftarrow 2k - 1$
    $q \leftarrow q_1$
    $r \leftarrow \frac{r}{p}$
  else
    $k \leftarrow 2k$
    $q \leftarrow q - q_1$
    $r \leftarrow \frac{r-p}{1-p}$
  end if
end for

The variable k gives the solution for (47). The computational cost is

$$O(L) = O(\log_2 N).$$

D.4 Update the table when some v_j changes

If one v_j changes, there is exactly one element in $\{s_{l,j}\}$ to be updated, for each l. Hence we need to update a total number of L summations in the table. More precisely, if we write the binary expansion of j,

$$j = \sum_{l=0}^{L} \beta_l 2^l,$$

we only need to update

$$s_{l,\alpha_l} := s_{l,\alpha_l} + v_j^{new} - v_j^{old}, \quad l = 0, \ldots, L,$$

where $\alpha_0 = 1$ and

$$\alpha_l = 2\alpha_{l-1} + \beta_{L+1-l} - 1.$$

This cost is also $O(\log_2 N)$.